Sex-dependent effects of preconception exposure to arsenite on gene transcription in parental germ cells and on transcriptomic profiles and diabetic phenotype of offspring

Abhishek Venkatratnam[1,2] · Christelle Douillet[1] · Brent C. Topping[2] · Qing Shi[1] · Kezia A. Addo[2] · Folami Y. Ideraabdullah[1,3] · Rebecca C. Fry[2] · Miroslav Styblo[1]

Received: 11 June 2020 / Accepted: 20 October 2020 / Published online: 3 November 2020

Abstract

Chronic exposure to inorganic arsenic (iAs) has been linked to diabetic phenotypes in both humans and mice. However, diabetogenic effects of iAs exposure during specific developmental windows have never been systematically studied. We have previously shown that in mice, combined preconception and in utero exposures to iAs resulted in impaired glucose homeostasis in male offspring. The goal of the present study was to determine if preconception exposure alone can contribute to this outcome. We have examined metabolic phenotypes in male and female offspring from dams and sires that were exposed to iAs in drinking water (0 or 200 μg As/L) for 10 weeks prior to mating. The effects of iAs exposure on gene expression profiles in parental germ cells, and pancreatic islets and livers from offspring were assessed using RNA sequencing. We found that iAs exposure significantly altered transcript levels of genes, including diabetes-related genes, in the sperm of sires. Notably, some of the same gene transcripts and the associated pathways were also altered in the liver of the offspring. The exposure had a more subtle effect on gene expression in maternal oocytes and in pancreatic islets of the offspring. In female offspring, the preconception exposure was associated with increased adiposity, but lower blood glucose after fasting and after glucose challenge. HOMA-IR, the indicator of insulin resistance, was also lower. In contrast, the preconception exposure had no effects on blood glucose measures in male offspring. However, males from parents exposed to iAs had higher plasma insulin after glucose challenge and higher insulinogenic index than control offspring, indicating a greater requirement for insulin to maintain glucose homeostasis. Our results suggest that preconception exposure may contribute to the development of diabetic phenotype in male offspring, possibly mediated through germ cell-associated inheritance. Future research can investigate role of epigenetics in this phenomenon. The paradoxical outcomes in female offspring, suggesting a protective effect of the preconception exposure, warrant further investigation.

Keywords Arsenic · Preconception exposure · Gene transcription · Germ cells · Sex dependent · Diabetes · Mice

Electronic supplementary material The online version of this article (https://doi.org/10.1007/s00204-020-02941-w) contains supplementary material, which is available to authorized users.

✉ Rebecca C. Fry
rfry@email.unc.edu

✉ Miroslav Styblo
styblo@med.unc.edu

[1] Department of Nutrition, CB# 7461, Gillings School of Global Public Health, University of North Carolina at Chapel Hill, Chapel Hill, NC 27599-7461, USA

[2] Department of Environmental Sciences and Engineering, CB#7431, Gillings School of Global Public Health, University of North Carolina at Chapel Hill, Chapel Hill, NC 27599-7431, USA

[3] Department of Genetics, CB#7264, School of Medicine, University of North Carolina at Chapel Hill, Chapel Hill, NC 27599-7264, USA

Introduction

Type 2 diabetes is a prevalent medical condition that poses a significant public health concern. According to the 2020 National Diabetes Statistics Report, nearly 34.2 million in the United States are affected by this chronic disease (CDC 2020). Exposure to chemicals and other environmental factors has been shown to contribute to the increasing prevalence of diabetes (Ardisson Korat et al. 2014; Thayer et al. 2012). The etiology of type 2 diabetes is complex and can elicit multiple factors, including genetics and environment interactions (Romao and Roth 2008).

Inorganic arsenic (iAs) is a ubiquitous environmental metalloid that is present in drinking water, soil, food, and other consumer products (Chung et al. 2014). In drinking water, levels of iAs are shown to exceed the WHO limit of 10 µg As/L in many regions of the United States, Bangla-desh, India, China, and Taiwan, and parts of South Amer-ica (Naujokas et al. 2013; WHO 2017). Chronic exposure to iAs is associated with cancer and other adverse health outcomes (Abdul et al. 2015; Kapaj et al. 2006; Maull et al. 2012). Diabetogenic effects of iAs exposures have been well studied in both humans and rodents (Maull et al. 2012). In humans, many epidemiological studies world-wide have linked iAs exposures with diabetes (Lai et al. 1994; Navas-Acien et al. 2008; Rahman et al. 1998; Tseng et al. 2000). In mice, iAs is shown to impair glucose home-ostasis with or without dietary modifications (Castriota et al. 2020; Liu et al. 2014; Paul et al. 2007, 2011). Several molecular mechanisms for iAs-induced glucose dysregulation have been reported. These include oxidative stress, epigenetic alterations, and inflammatory signaling (Beck et al. 2017; Carmean and Seino 2019; Martin et al. 2017; Tseng 2004). IAs exposure is also associated with insulin resistance and β-cell dysfunction in both humans and mice (Douillet et al. 2013; Grau-Perez et al. 2017; Liu et al. 2014; Padmaja Divya et al. 2015). A postulated underly-ing mechanism for arsenic-dependent insulin resistance is the down-regulation of the insulin-stimulated protein kinase B (Akt) signaling pathway (Paul et al. 2011; Walton et al. 2004; Zhang et al. 2017), while impaired mitochon-drial metabolism and inhibition of calcium influx appear to underlie the inhibition of insulin secretion by β-cells (Dover et al. 2018a, b; Huang et al. 2019). In humans, exposure to iAs often occurs over a lifetime; however, diabetogenic effects of iAs exposure at specific develop-mental windows, including exposure of parental germ cells prior to conception, has never been systematically exam-ined. Some data in humans (Kile et al. 2014; Rager et al. 2014; Rojas et al. 2015) and mice (Fry et al. 2019; Huang et al. 2018) suggest that prenatal exposures play a role in diabetes development in offspring. But the specific role of preconception exposure alone on phenotypic outcomes in the offspring remains unclear.

The present study focuses on characterizing gene expression changes in germline cells from parental mice exposed to iAs as a potential mechanism by which preconception exposure to iAs may alter metabolic phenotypes in offspring. We hypothesized that preconception exposure to iAs would lead to changes in transcript levels in parental germline cells and in an adverse metabolic phenotype in offspring. We further hypothesized that offspring target tissue transcription profiles would reflect the preconception-associated germline transcription. To address this hypothesis, we conducted metabolic phenotyping and tissue-specific RNA sequencing in male and female offspring from parents that were exposed to iAs prior to conception. Our study highlights novel findings that suggest the preconception iAs exposure plays a role in glucose dysregulation in adult mice in a sex-specific manner.

Materials and methods

Preconception exposure to iAs

All procedures involving mice were approved by the UNC Institutional Animal Care and Use Committee. Twenty male and 40 female C57BL/6J mice (6 weeks old) were purchased from the Jackson Laboratory (Bar Harbor, ME) and housed in the UNC animal facilities. All mice were singly caged upon arrival. The housing room was set on a 12-h light–dark cycle. The experimental design of the study is shown in Fig. 1. All mice were left to acclimatize for 2 weeks while fed AIN-93G food pellets (Research Diets Inc., New Brunswick, NJ) and drank arsenic-free deionized water (DIW). After acclimatization, all mice were arbitrarily separated into two exposure groups. Twenty female and 10 male mice were exposed to sodium arsenite in deionized water (200 µg As/L, ppb) for 10 weeks. The remaining animals in the second, control group continued drinking DIW. Sodium arsenite (> 99% pure) was purchased from Sigma Aldrich (St. Louis, MO). Drinking water in both groups was changed weekly. Water consumption was recorded on a weekly basis; food consumption was monitored every 2 weeks. The body weights were monitored biweekly. On week 9 of exposure, mice were fasted for 6 h, and tail bleeds were performed to measure fasting blood glucose (FBG) and fasting plasma insulin (FPI). After week 10, iAs exposure was terminated, and ten male and ten female mice from each treatment group were mated (one on one) for 1 week. During this time, all mice drank DIW. The ten remaining female mice in each treatment group were sacrificed, and oocytes were collected from ovaries. Following the mating period, the males were also sacrificed, and sperm was collected from

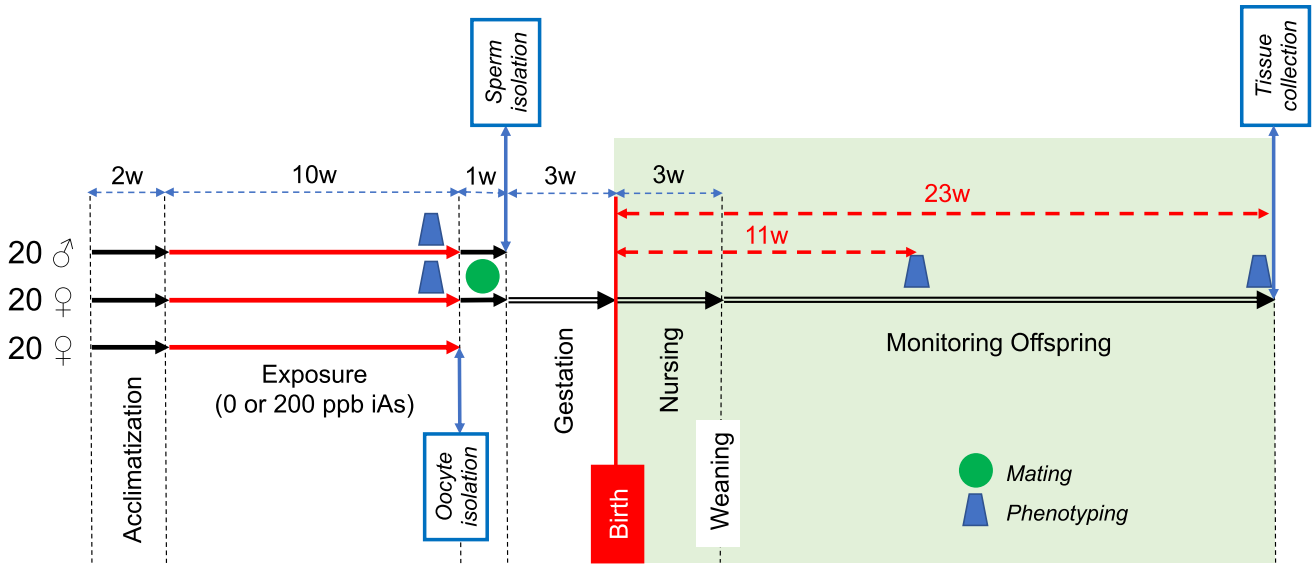

Fig. 1 Experimental design. After acclimatization for 2 weeks, 20 male and 2×20 female mice were exposed to 0 or 200 ppb iAs in drinking water for 10 weeks. Phenotyping was performed at week 9. At week 10, oocytes were isolated from ten females after sacrifice. The remaining ten females and ten males were mated (one on one) for 1 week. After mating, sperm was collected from males. Offspring born to pregnant dams were weaned at age of 3 weeks. Phenotype of the offspring was examined at age of 11 and 23 weeks. Tissues were collected from 23-week-old offspring after sacrifice

cauda epididymis. (The methods used for oocyte and sperm isolation are described below.) The mated females were singly housed and closely monitored for pregnancy and pup births.

Offspring

At weaning (i.e., at 22 days of age), the G1 mice (the offspring) were weighed and singly housed. All G1 mice drank DIW ad libitum and were fed the AIN-93G diet. The body weights, food, and water consumption were monitored as described for the parental generation. Magnetic resonance imaging (MRI) using Echo MRI three-in-one Composition Analyzer and Labmaster (Echo Medical Systems, Houston, TX, USA) was conducted at 11 and 23 weeks of age to determine body composition (%fat and %lean mass). Metabolic phenotypes were also assessed at 11 and 23 weeks of age. Specifically, FBG and FPI were measured after 6-h fasting. Fasted mice were then injected intraperitoneally with D-glucose (Sigma Aldrich, St. Louis, MO) in phosphate-buffered saline (2 g glucose/kg b.w.) and blood glucose and plasma insulin were measured 15 min post-dosing. After completion of the phenotype analysis at 23 weeks of age, mice were euthanized by cervical dislocation. Pancreatic islets were isolated as described below. The islets, along with other tissues collected after sacrifice, were flash frozen and stored at − 80 °C.

Analysis of blood glucose and plasma insulin

For both parental generation and the offspring, blood (~ 100 µL) was collected from tail cuts in ammonium heparin-coated capillary tubes from Kimble (Dover, Ohio). Glucose levels were measured in whole blood by One Touch® Ultra® glucometer (LifeScan, Inc., Milpitas, CA). Plasma was isolated by centrifugation at 1700×*g* for 15 min at 4 °C and stored at − 80 °C. Plasma insulin levels were measured using ELISA kits from Crystal Chem (Elk Grove Village, IL) following the manufacturer's protocol.

Calculation of metabolic indices

Homeostasis assessment-insulin resistance (HOMA-IR) index, an indicator of insulin resistance, was calculated using FBG (mg/dL) and FPI (µU/mL) as follows: HOMA-IR = [(FBG) × (FPI)]/405. FBG was expressed in mmol/mL for calculation of HOMA-β cell function (HOMA-B) index using the equation HOMA-B = [FPI × 20]/[FBG − 3.5]. The insulinogenic index, an indicator of β cell function in response to glucose challenge, was calculated as $(FPI_{15min} - FPI_{Basal})/(FBG_{15min} - FBG_{Basal})$.

Oocyte collection

The oocytes were collected by manual extraction methods from the ten control and ten iAs-exposed females that were not involved in mating. The media required to

collect oocytes was freshly prepared before organ harvests. Minimum essential medium (MEM) Eagle's media, sodium bicarbonate, polyvinylpyrrolidone (PVP), sodium pyruvate, 1 M HEPES buffer, gentamycin (50 mg/mL), and Milrinone, a blood vessel vasodilator, were purchased from either Sigma Aldrich (St. Louis, MO) or Fischer Scientific (Hampton, NH). In brief, 90 mL of MEM media was taken in a beaker, and 0.22 g of sodium bicarbonate was added to it. 0.3 g of PVP and 0.01 g of sodium pyruvate were added to the above solution. 2.5 mL of 1 M HEPES and 0.1 mL of gentamycin (50 mg/mL) were aliquoted to the above solution. The pH was adjusted to 7.3, and the prepared media was made up to 100 mL and transferred to a bottle wrapped in foil and placed in a water bath maintained at 37 °C. 2.5 mM of milrinone was added to the media to prevent oocyte maturation. Media containing milrinone was transferred to a 60 × 15-mm Petri dish. Ovaries were isolated during necropsy and separated from surrounding adipose tissues. The clean ovaries were then placed in the Petri dish with media. Using $25^{5/8}$ G syringe needles, ovaries were shredded under a Nikon SMZ 800 N microscope (Minato, Tokyo). A mouth pipette was assembled with a silicon tip from Drummond Scientific Company (Broomall, PA). The other end of the silicon tip was attached to a stripper or capillary plastic tube with an internal diameter of 75 µm from Cooper Surgical Inc. (Trumbull, CT). The mouth pipette setup was used to strip cumulous cells and other debris from oocytes by pipetting back and forth. The oocytes were then transferred into an Eppendorf tube containing RNase inhibitor (Qiagen, MD) and placed on dry ice.

Sperm collection

Sperm was collected using the swim out method from ten sires immediately after 1 week of mating. The buffer for sperm collection was freshly prepared before necropsy. Human Tubal Fluid (HTF) HEPES buffer was purchased from Fisher Scientific (Hampton, NH). Bovine serum albumin (BSA) was purchased from Sigma Aldrich (St. Louis, MO). BSA was added to the buffer so that the final concentration was 5 mg/mL. The vas deferens and cauda epididymis were transferred into 1 mL of warm 1X HTF on a well plate. Using a $26^{1/2}$ G syringe needle, the vas deferens and epididymis were thoroughly scored to release sperm cells into the media. The media was incubated for 10 min at 37 °C incubator to allow sperm to swim out to the media. The media was then transferred to a 1.5-mL Eppendorf tube and centrifuged at 12,000*g* for 5 min. The supernatant was removed, and the pellet containing the sperm cells was frozen in dry ice.

Isolation of pancreatic islets

Islets were isolated from pancreata of male and female offspring using the previously described in situ collagenase perfusion method followed by centrifugation in Ficoll PM 400 (GE Healthcare, Uppsala, Sweden) (Douillet et al., 2013). Collagenase P was purchased from Roche Diagnostics Corp. (Indianapolis, IN). The islets were washed with Hank's balanced Salt Solution containing 10 mM HEPES, 7.5% sodium bicarbonate and 0.25% BSA (all from Sigma Aldrich); pH was adjusted to 7.4.

RNA sequencing and differential gene expression analysis in sperm and oocytes from parental mice

Sperm and oocyte samples, five per treatment group, were selected from the parental generation for RNA sequencing. Total RNA extraction, library preparation, sequencing, and reads alignment was conducted at the UNC Center for Gastrointestinal Biology and Disease (CGIBD) Advanced Analytical Core. SMART-seq v4 Ultra Low RNA kit was purchased from TaKaRa Bio USA, Inc. (Mountain View, CA) for RNA extraction. cDNA libraries were prepared using Nextera XT DNA Library Preparation Kit from Illumina® (San Diego, CA). Sequencing was conducted using NextSeq 500/500 v2.5 (150 cycles) kits from Illumina® (San Diego, CA). Reads were aligned to the mm9 genome using Spliced Transcripts Alignment to a Reference (STAR) (Dobin et al. 2013). Differential gene expression was assessed using the DESeq package (Love et al. 2014). Transcriptome data were filtered to genes with absolute read counts of more than 10 in all sperm and oocyte samples for differential gene expression analysis (Venkatratnam et al. 2018). Differentially expressed genes were identified based on Benjamini–Hochberg FDR < 0.1. Pathway analysis was conducted using the Database for Annotation, Visualization and Integrated Discovery (DAVID) (Dennis et al. 2003; Huang et al. 2009). The differentially expressed genes with p values < 0.05 were used for pathway analyses.

RNA sequencing and differential gene expression analysis in pancreatic islets and livers from offspring

RNA sequencing was carried out in islets from three male and five female offspring from the control parents and five male and five female offspring from iAs-treated parents. RNA sequencing was also carried out in livers from five male and six female offspring from control parents and five male and five female offspring from iAs-treated parents. RNA was extracted from islets using RNAqueous micro kit from Ambion® (Austin, TX). cDNA libraries were prepared using SEQuoia Complete Stranded RNA Library Kit from Bio-Rad laboratories (Hercules, CA). RNA from

livers was extracted using RNeasy mini kit from Qiagen (Germantown, MD). cDNA libraries were prepared using Next Ultra II Directional RNA Library Prep Kit from New England Biolabs Inc (Ipswich, MA). Islet and liver RNA was sequenced using NextSeq 500/500 v2.5 (77 cycles) kits from Illumina® (San Diego, CA). Reads alignment, differential gene expression, and pathway analysis were conducted as described above.

Data analysis of phenotypic endpoints

GraphPad Prism (La Jolla, CA) and R studio (Boston, CA) were used for data analysis and visualizations. Data from metabolic phenotyping were screened for outliers using Grubb's outlier test. These data are presented in scatterplots graphs where the bars represent the mean and standard deviation. The data represent observations in male ($N = 10, 25$) and female ($N = 10, 28$) control and iAs nests. Mann–Whitney non-parametric test was used to characterize differences between treatment groups and sexes; $p < 0.05$ was used as a threshold for statistical significance.

Results

Phenotypic characteristics of the parental mice

No statistically significant difference in FBG and FPI were observed between control and iAs-exposed males or females from the parental generation (Suppl. Figure 1A, B, C, D). Similarly, no treatment-related differences were found in HOMA-IR and HOMA-B (Suppl. Figure 1E, F, G, H).

Transcriptomic responses in sperm cells and oocytes of parental mice exposed to iAs

Gene expression profiles were examined in the oocytes that were collected from the control and iAs-exposed virgin females and in the sperm collected from control and iAs-exposed sires after mating. RNA sequencing identified 912 and 180 genes differentially expressed in response to iAs exposure ($p < 0.05$) in sperm cells and oocytes, respectively (Suppl. Tables 1 and 2). After false discovery rate correction using Benjamini–Hochberg method, five genes were identified to show altered expression due to iAs exposure in sperm cells, namely protein tyrosine phosphatase non-receptor type 22 (*Ptpn22*), cluster of differentiation 240 (*Cd240*), chemokine (C–C motif) ligand 8 (*Ccl8*), major vault protein (*Mvp*), and ras-related protein (*Rab3d*) were statistically significant (FDR < 0.1) (Table 1). Interestingly, no statistically significant effects of iAs exposure on gene expression in oocytes were found at FDR < 0.1. Pathway enrichment analysis was conducted using DAVID via the KEGG and BioCarta pathways. The genes ($n = 912$; $p < 0.05$) altered by iAs exposure in sperm cells have known roles in several biological pathways including Focal adhesion, Insulin-like growth factor binding, Phosphoinositide 3 kinase/protein kinase B (PI3K-Akt) signaling, extracellular matrix receptor interaction, and Wingless-related integration site (Wnt) signaling that were significantly perturbed (FDR < 0.1) and are relevant to glucose dysregulation (Table 2). No statistically significant pathway perturbation was observed in oocytes.

Numbers and sex of the offspring

Nine out of ten dams exposed to iAs prior to mating gave birth to offspring. In contrast, the mating of ten control pairs resulted only in three litters (Suppl. Table 3). Thus, the G1 generation consisted of 10 females and 10 males from the control parents and 29 females and 27 males from iAs-treated parents. Two males and one female from iAs-treated parents died later after weaning for unknown causes.

Table 1 Genes that were differentially expressed in sperm cells of sires exposed to iAs

Gene	Base mean	Log_2 fold change	*p* value	Benjamini–Hochberg adjusted *p* value
Protein tyrosine phosphatase, non-receptor type 22 *(Ptpn22)*	133.95	− 0.90	6.38E−06	0.05
Cluster of differentiation *(CD248)*	84.67	1.28	1.12E−05	0.05
Chemokine (C–C motif) ligand 8 *(Ccl8)*	297.20	1.04	1.84E−05	0.05
Major vault protein *(Mvp)*	231.27	0.48	2.13E−05	0.05
Ras-related protein Rab-3D *(Rab3d)*	145.55	0.58	4.35E−05	0.08

Sperm was collected after mating from males exposed to iAs for 10 weeks prior to mating and unexposed control males. Differentially expressed genes were identified based on Benjamini–Hochberg adjusted *p* value < 0.1

Table 2 Top pathways in sperm cells that were significantly enriched for genes ($n = 912$) altered by exposure to iAs

Category	Pathway	Fold enrichment	p value	Benjamini–Hochberg adjusted p value
KEGG	Focal adhesion	3.25	9.71E−08	2.43E−05
KEGG	PI3K-Akt signaling pathway	2.53	3.57E−07	4.46E−05
KEGG	ECM-receptor interaction	3.82	6.08E−05	0.005
Gene ontology	Collagen trimer	4.05	3.59E−05	0.001
Gene ontology	Insulin-like growth factor binding	8.35	2.84E−05	0.006
Gene ontology	Positive regulation of non-canonical Wnt signaling	19.54	4.57E−05	0.024

Differentially expressed genes ($p < 0.05$) were analyzed for pathways enrichment; the significantly enriched pathways were identified using a Benjamini–Hochberg adjusted p value < 0.1

Phenotypic characteristics of the G1 offspring

Food and water consumption, and body weights

Body weights of the offspring were monitored weekly from weaning (i.e., week 3 of age) until week 23 of age. During this period, male and female mice in both treatment groups steadily gained weight (Suppl. Figure 2A). Male mice were heavier compared to females by the end of the study. There were no statistically significant differences between males or females due to treatment. Food and water consumption were relatively steady for most duration of the study. Food consumption varied between 2.5 and 3.5 g/day and tended to be higher in males as compared to females (Suppl. Figure 2B). Water consumption ranged from 2.5 to 6.2 g/day (Suppl. Figure 2C).

Body composition

At 11 weeks of age, no significant differences were detected in body composition (% fat and % lean mass) between the treatment groups or between males and females within each treatment group (Suppl. Figure 3). At 23 weeks of age, no treatment-related differences were found in body composition of G1 males (Fig. 2a, c); however, females from the iAs-exposed parents had significantly higher % fat than females from the control parents ($p = 0.01$) (Fig. 2b). There were no significant treatment-related differences in % lean mass among G1 females (Fig. 2d). At 23 weeks of age, G1 males had significantly higher % fat than females in the treatment group ($p = 0.0003$), but not in the control group ($p = 0.052$) (Fig. 2a, b). At this age, % lean mass in G1 females were significantly ($p = 0.0092$) higher than in males within the iAs-exposed parental group (Fig. 2c, d).

Blood glucose and plasma insulin

FBG and FPI, as well as blood glucose and plasma insulin levels 15 min after glucose challenge were measured at 11 and 23 weeks of age. At week 11, there were only few significant differences in the glucose and insulin measures between treatment groups or between sexes (Suppl. Figure 4). Specifically, FBG was lower in females from iAs-treated parents than in females from control parents ($p = 0.039$); Δ glucose$_{(15–0\text{min})}$ value (i.e., the difference between 15-min glucose and FBG) was greater in males from iAs-exposed parents as compared to males from control parents ($p = 0.028$). The same differences were found in the offspring at 23 weeks of age, but at this time point, these differences were not statistically significant: $p = 0.07$ for the difference in FBG in females and $p = 0.09$ for the difference in Δ glucose$_{(15–0\text{min})}$ in males (Suppl. Figure 5). However, a statistically significant difference was found in 15-min blood glucose among the female offspring; 15-min glucose was lower in females from iAs-treated parents (Suppl. Figure 5D). At 23 weeks, 15-min plasma insulin was higher in males from iAs-exposed parents as compared to controls ($p = 0.02$) (Suppl. Figure 6). In contrast, no statistically significant treatment-related differences were found among the female offspring.

Since we found that % fat differed significantly between females from the control and iAs-treated parents and because adiposity is known to affect blood glucose and insulin levels, we re-assessed the differences in blood glucose and plasma insulin levels at week 23 while normalizing for % fat. We found that the normalized FBG, 15-min glucose, and Δ glucose$_{(15–0\text{ min})}$ were significantly lower ($p < 0.025$) in females from the iAs-treated nests as compared to females from the control nests (Fig. 3b, d, f). There were no statistically significant treatment-related differences in the glucose measures among males (Fig. 3a, c, e). The normalized FPI and 15-min plasma insulin were found to be lower in females from the iAs-treated parents than in those from the control parents (Fig. 4a, b) with $p = 0.074$ and $p = 0.017$, respectively. Differences were also found in the normalized 15-min insulin ($p = 0.003$) and Δ insulin$_{(15–0\text{min})}$ ($p = 0.07$) among male offspring; both values were higher in males from the iAs-treated parents (Fig. 4c, d).

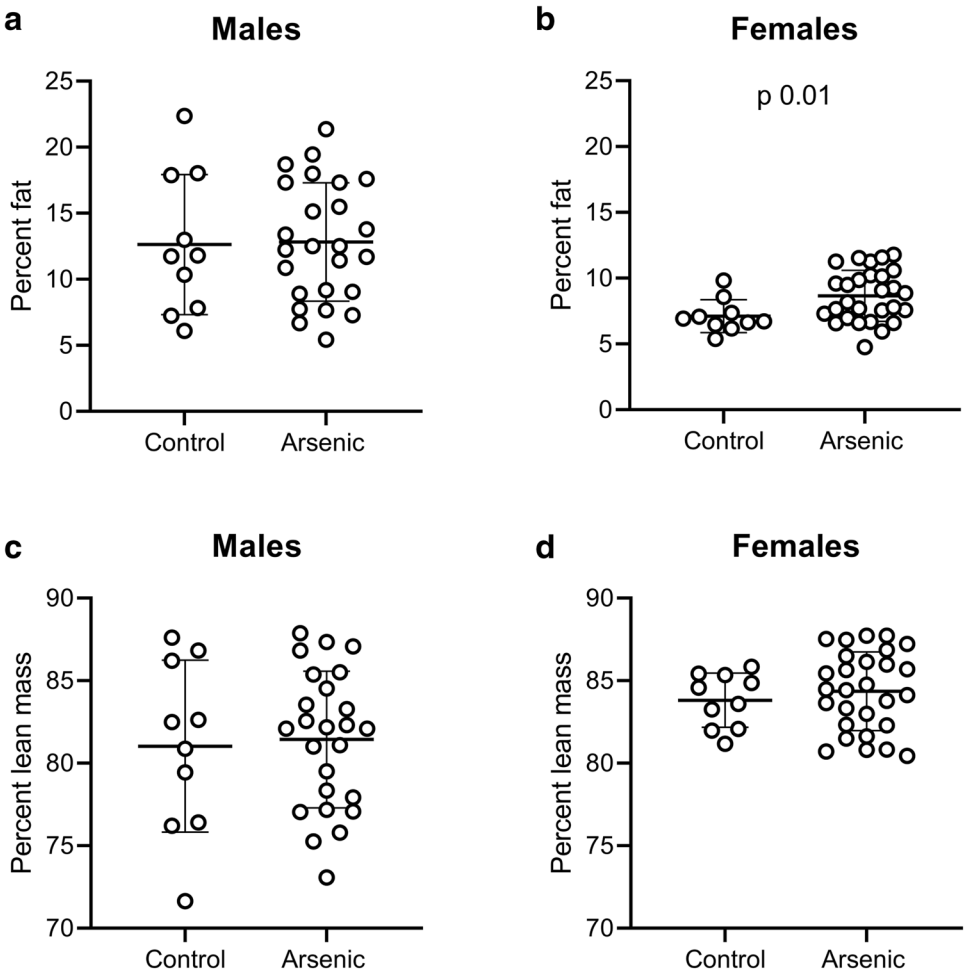

Fig. 2 Body composition of 23-week-old male and female offspring from parents exposed to iAs prior to mating and from control, unexposed parents: percent body weigh represented by fat (percent fat) in male (**a**) and female (**b**) offspring, and percent body weight represented by lean mass (percent lean mass) in male (**c**) and female (**d**) offspring. Scatter plots show mean, ± SD and individual values. p values for the statistically significant differences ($p < 0.05$) between treatments are shown

While focusing on the effects of iAs exposure, we also found statistically significant differences between males and female offspring within each treatment group. Specifically, the normalized FBG was significantly higher in females compared to males regardless of treatment ($p = 0.0082$). The normalized 15-min glucose and normalized Δ glucose$_{(15–0min)}$ were significantly higher in females than males from the control parents ($p = 0.007$). The normalized 15-min plasma insulin was significantly higher in females than males from the control parents ($p = 0.0288$), but was significantly lower in females than males from the iAs-treated parents ($p = 0.0007$). The normalized Δ insulin$_{(15–0min)}$ was higher in males compared to females from the iAs-treated parent, but this difference did not reach statistical significance ($p = 0.0522$).

Insulin resistance and β-cell function

We used FBG and FPI values to calculate HOMA-IR, an indicator of insulin resistance, and HOMA-B, an indicator of β-cell function. Insulinogenic index was calculated to evaluate β-cell function after glucose challenge. We found no statistically significant differences in HOMA-IR or HOMA-B values among the treatment groups (Suppl. Figure 7). However, the insulinogenic index was higher in males from iAs-treated parents as compared to controls ($p = 0.05$); no difference was found among females (Suppl. Figure 7E, F). When normalized for % fat HOMA-IR was found to be significantly lower in females from the iAs-treated parents as compared to the control parents ($p = 0.04$) (Fig. 5b), no significant differences were found in the normalized HOMA-B or insulinogenic index (Fig. 5d, f). In contrast, the preconception exposure had no significant effects on the normalized HOMA-IR and HOMA-B in the male offspring (Fig. 5a, c). However, the normalized insulinogenic index for males from the iAs-treated parents was significantly higher than for males from the control parent ($p = 0.0269$) (Fig. 5e). Sex-related differences were found only among offspring from iAs-treated parents. The normalized HOMA-IR was significantly higher in males compared to females ($p = 0.0287$) and normalized HOMA-B was higher in females than males ($p = 0.0234$). In addition, the normalized insulinogenic index was significantly higher in males compared to females ($p = 0.0473$).

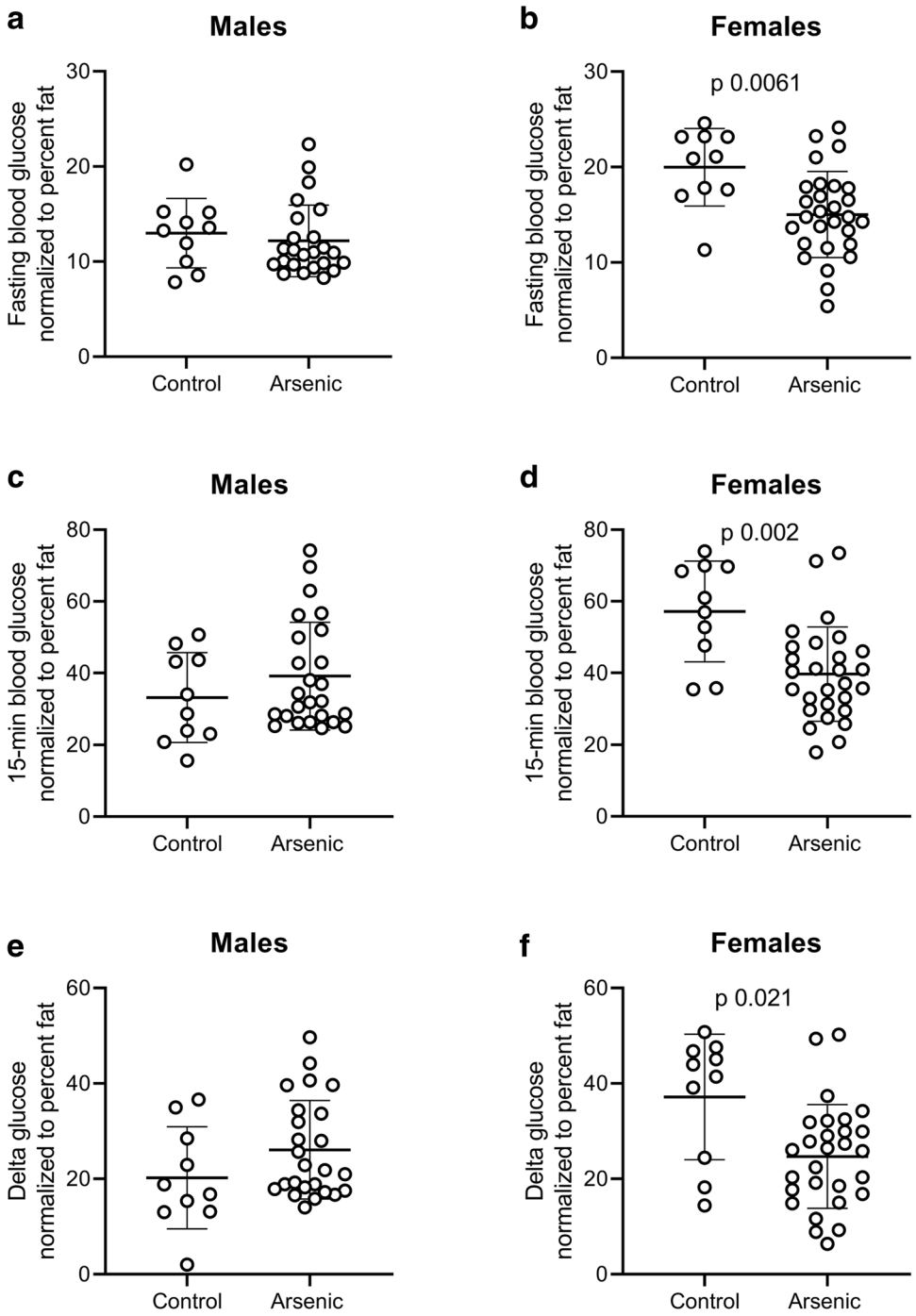

Fig. 3 Fasting blood glucose (**a**, **b**), 15-min blood glucose (**c**, **d**) and delta glucose (i.e., 15-min glucose – fasting glucose) (**e**, **f**) normalized to percent body fat in 23-week-old male and female offspring from iAs-treated and control parents. Scatter plots show mean, ± SD and individual values. *p* values for the statistically significant differences ($p < 0.05$) between treatments are shown

Transcriptomic responses in islets and livers of male and female offspring from iAs-treated parents

We compared transcript levels in the islets and livers of male and female offspring from iAs-treated parents to those in the islets and livers of the control offspring using RNA sequencing.

In the islets of female and male offspring, 99 and 100 genes were differentially expressed in response to the preconception iAs exposure ($p < 0.05$), respectively (Suppl. Tables 4 and 5). However, no statistically significant differences between the transcript levels in the islets from the control and treatment groups were found after adjusting for multiple testing using Benjamini–Hochberg method. Pathway enrichment analysis of the $n = 100$ differentially expressed genes ($p < 0.05$) identified multiple pathways altered by the preconception exposure to iAs in male islets; pathways involved in translational processes were among the

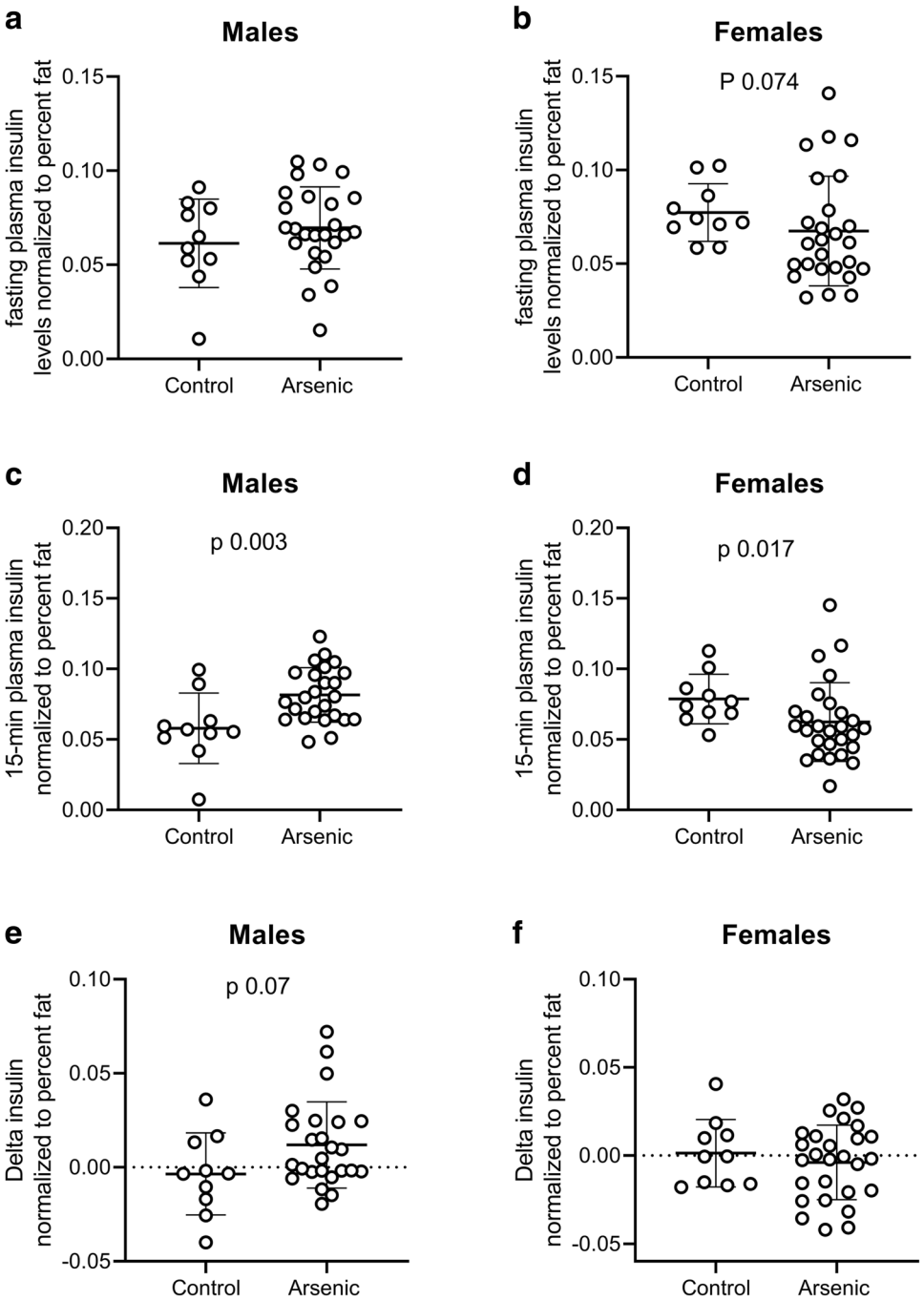

Fig. 4 Fasting plasma insulin (**a**, **b**), 15-min plasma insulin (**c**, **d**), and delta insulin (i.e., 15-min insulin–fasting insulin) (**e**, **f**) normalized to percent body fat in 23-week-old male and female offspring from iAs-treated and control parents. Scatter plots show mean, ± SD, and individual values. *p* values for the statistically significant differences ($p < 0.05$) are shown along with *p* values that are higher than 0.05 but lower than 0.1

most significantly affected (FDR < 0.1) (Suppl. Table 6). No pathways were significantly altered in female islets.

In the liver, the transcriptomic responses were considerably stronger than in the islets. The preconception exposure altered 1407 and 843 genes significantly ($p < 0.05$) in the livers of the female and male offspring, respectively (Suppl. Tables 7 and 8). After adjusting for false discovery rates, eight genes in the female livers, and one gene in the male livers were found to be significantly perturbed (FDR < 0.1) (Table 3). In female livers, these genes included AarF domain containing kinase 5 *(Adck5),* Hydroxypyruvate isomerase *(Hyi),* BTG3-associated nuclear protein *(Banp),* ATP-binding cassette sub-family A member 9 *(Abca9),* Cytochrome B-245 beta chain *(Cybb),* Ubiquitin-like modifier activating enzyme 6 *(Uba6),* ADP ribosylation factor Like GTPase 4D *(Arl4d),* and Asparaginase *(Aspg).* Expression of G0/G1 switch gene 2 *(G0s2)* was found to be altered in male livers. Pathway analysis using differentially expressed genes with *p* values < 0.05 ($n = 843$) identified several pathways that were altered in

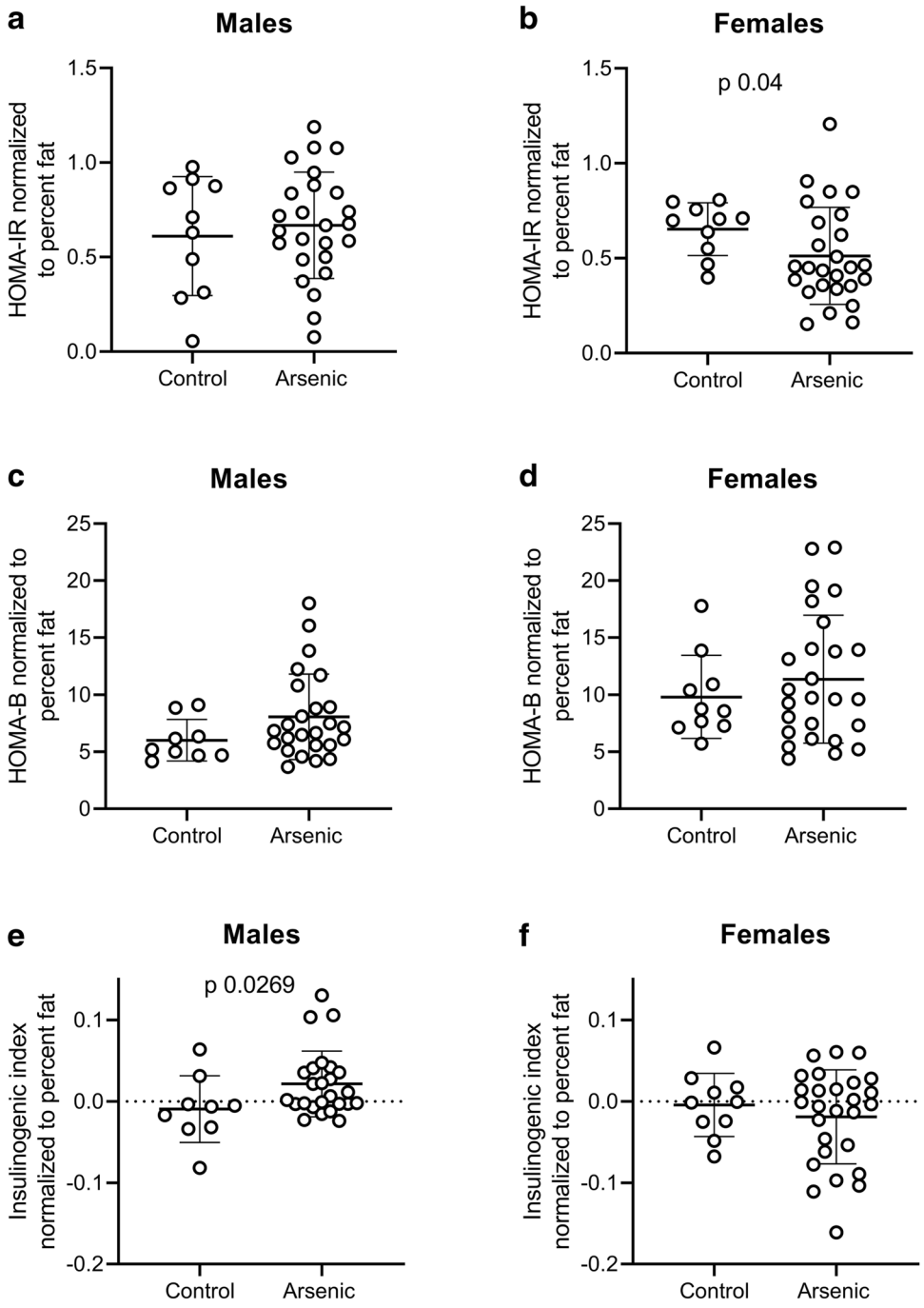

Fig. 5 HOMA-IR (**a**, **b**), HOMA-B (**c**, **d**), and insulinogenic index (**e**, **f**) normalized to percent body fat in 23-week-old male and female offspring from iAs-treated and control parents. Scatter plots show mean, ± SD, and individual values. *p* values for the statistically significant differences ($p < 0.05$) between treatments are shown

male livers by the preconception iAs exposure, including extracellular matrix (ECM) receptor interaction, focal adhesion, and PI3K-Akt signaling pathways (Table 4). The differentially expressed genes in female livers ($n = 1407$) were enriched in pathways associated, for example, with ribosomal structure and function, with mitochondrial respiration and oxidative phosphorylation, non-alcoholic fatty liver disease, and NADH dehydrogenase activity (Table 5).

Genes differentially expressed in both the parental germ cells and the tissues of the offspring

We compared genes that were differentially expressed in the parental germline cells with genes differentially expressed in the islets and livers of the offspring using the $p < 0.05$ threshold. We identified 95 genes in livers of male and 81 genes in livers of female offspring that were also

Table 3 Genes that were differentially expressed ($n=9$) in livers of female and male offspring from parents exposed to iAs

Gene (male livers)	Base mean	Log_2 fold change	p value	Benjamini–Hochberg adjusted p value
G0/G1 switch gene 2 *(G0s2)*	2364.91	− 1.820	7.91E−06	0.087
Gene (female livers)	Base mean	Log_2 fold change	p value	Benjamini–Hochberg adjusted p value
AarF domain containing kinase 5 *(Adck5)*	550.79	− 0.74029	5.69E−07	0.006271
Hydroxypyruvate isomerase *(Hyi)*	1062.55	− 0.77357	2.42E−06	0.008925
BTG3-associated nuclear protein *(Banp)*	209.52	− 1.01104	2.43E−06	0.008925
ATP-binding cassette sub-family A member 9 *(Abca9)*	80.86	0.732965	1.49E−05	0.040947
Cytochrome B-245 beta chain *(Cybb)*	465.07	0.619609	1.86E−05	0.041049
Ubiquitin-like modifier activating enzyme 6 *(Uba6)*	112.97	0.788383	5.34E−05	0.097647
ADP ribosylation factor Like GTPase 4D *(Arl4d)*	349.28	− 0.71922	7.06E−05	0.097647
Asparaginase *(Aspg)*	3185.9	− 0.42721	7.09E−05	0.097647

Differentially expressed genes were identified based on Benjamini–Hochberg adjusted p value < 0.1

Table 4 Top pathways in livers of male offspring that were significantly enriched for genes ($n=843$) altered by preconception exposure to iAs[a]

Category	Pathway	Fold enrichment	p value	Benjamini–Hochberg adjusted p value
KEGG	Focal adhesion	2.69	9.71E−06	0.001
KEGG	ECM-receptor interaction	3.41	1.90E−04	0.006
KEGG	PI3K-Akt signaling pathway	1.89	8.38E−04	0.023
Gene ontology	Cell cycle	1.98	8.46E−06	0.006
Gene ontology	Platelet-derived growth factor binding	12.32	6.73E−05	0.011
Gene ontology	Extracellular matrix structural constituent	5.40	2.04E−04	0.017
KEGG	Protein digestion and absorption	2.92	0.002381	0.049
Gene ontology	Collagen trimer	3.052	0.005332	0.079
Gene ontology	Leukocyte cell–cell adhesion	8.29	3.11E−05	0.014
Gene ontology	Membrane to membrane docking	19.89	6.07E−04	0.086
Gene ontology	ATP binding	1.45	2.92E−04	0.023
Gene ontology	Nucleotide binding	1.38	3.37E−04	0.024
Gene ontology	Cadherin binding involved in cell–cell adhesion	2.20	4.45E−04	0.027
Gene ontology	Cell–cell adherens junction	2.00	0.00175	0.031
Gene ontology	MCM complex	14.07	2.58E−04	0.007
Gene ontology	DNA unwinding involved in DNA replication	12.43	4.46E−04	0.070
KEGG	DNA replication	4.29	0.004963	0.086
Gene ontology	Chromosome condensation	9.32	3.11E−04	0.061
Gene ontology	Membrane to membrane docking	19.89	6.07E−04	0.086
KEGG	Bladder cancer	5.23	8.46E−05	0.005
Gene ontology	Phosphatidylinositol-3,4-bisphosphate binding	6.72	0.001597	0.071
Gene ontology	GO:0030261 ~ chromosome condensation	9.32	3.11E−04	0.061

Differentially expressed genes ($p<0.05$) were analyzed for pathways enrichment; the significantly enriched pathways were identified using a Benjamini–Hochberg adjusted p value < 0.1

differentially expressed in paternal sperm (Suppl. Tables 9 and 10). Similarly, we found 6 genes in male livers and 20 in female livers that were also differentially expressed in maternal oocyte (Suppl. Table 11). There were very few overlaps between genes differentially expressed in the germ cells and in the islets of the offspring (data not shown). We performed pathway analysis using genes that were differentially expressed in both paternal sperm and in livers of the male offspring ($n=95$) and female offspring ($n=81$). We identified 16 biological pathways in livers of the male offspring that were enriched for these genes (Table 6). As discussed below, some of these pathways are involved in

Table 5 Top pathways in livers of female offspring that were significantly enriched for genes ($n = 1407$) altered by preconception exposure to iAs

Category	Pathway	Fold enrichment	*p* value	Benjamini–Hochberg adjusted *p* value
Gene Ontology	Ribosome	4.55	4.07E−21	1.34E−18
KEGG	Ribosome	4.66	5.97E−20	1.57E−17
Gene ontology	Intracellular ribonucleoprotein complex	3.27	1.84E−17	3.02E−15
Gene ontology	Structural constituent of ribosome	3.42	4.95E−16	5.21E−13
Gene ontology	Translation	2.36	6.75E−10	2.36E−06
Gene ontology	Cytosolic large ribosomal subunit	3.83	1.64E−07	8.29E−06
Gene ontology	Mitochondrial inner membrane	3.19	6.91E−20	1.51E−17
Gene ontology	Respiratory chain	6.28	2.03E−12	1.67E−10
KEGG	Oxidative phosphorylation	3.74	3.56E−12	4.68E−10
Gene ontology	Mitochondrial respiratory chain complex I	6.74	1.73E−11	1.26E−09
KEGG	Parkinson's disease	3.40	1.40E−10	1.23E−08
KEGG	Huntington's disease	2.84	3.10E−09	1.63E−07
KEGG	Non-alcoholic fatty liver disease (NAFLD)	2.87	1.27E−07	5.55E−06
KEGG	Alzheimer's disease	2.70	2.06E−07	7.73E−06
Gene ontology	NADH dehydrogenase (ubiquinone) activity	4.98	4.07E−05	0.007
Gene ontology	NADH dehydrogenase activity	8.54	7.20E−05	0.011
Gene ontology	Cytosolic small ribosomal subunit	4.78	5.81E−07	2.72E−05
Gene ontology	Ribosomal small subunit assembly	7.41	2.59E−06	0.003
Gene ontology	Small ribosomal subunit	4.92	3.17E−04	0.009
Gene ontology	Peroxisome	3.02	2.03E−06	8.90E−05
KEGG	Peroxisome	3.39	3.72E−06	1.22E−04
Gene ontology	Peroxisomal membrane	3.29	0.001	0.038
KEGG	Valine, leucine and isoleucine degradation	3.07	0.001	0.040
Gene ontology	Proteasome complex	3.12	7.69E−04	0.020
Gene ontology	Sex chromatin	10.57	0.004	0.087

Differentially expressed genes ($p < 0.05$) were analyzed for pathways enrichment; the significantly enriched pathways were identified using a Benjamini–Hochberg adjusted p value < 0.1

the regulation of glucose homeostasis and/or are linked to pathologies associated with diabetes. No pathways were significantly enriched for the genes that were differentially expressed in the sperm and the livers of female offspring.

Discussion

The association between chronic iAs exposure from drinking water and type 2 diabetes has been supported by results of multiple cross-sectional and prospective population studies (Thayer et al. 2012). Almost all these studies have been carried out in adult cohorts, using the levels of iAs in drinking water at the time of the study as an indicator of iAs exposure. However, participants in many of these cohorts were likely exposed to iAs for a lifetime, and possibly across generations. Yet, no population study to date has systematically evaluated association between type 2 diabetes and prenatal exposure to iAs. Data from three recent studies suggest the iAs exposure during this developmental window may significantly contribute to the diabetogenic phenotypes observed in adults. In the first study, gestational iAs exposure was shown to alter CpG methylation of genes in cord blood of newborns in Bangladesh; some of these genes were associated with the Maturity onset diabetes of the young (Mody) pathway (Kile et al. 2014). Similarly, Rojas and associates showed that prenatal exposure to iAs-modified DNA methylation of 2919 genes in the cord blood of newborns in a birth cohort in Mexico (Rojas et al. 2015). Notably, for 16 of these genes the DNA methylation correlated with the transcript levels. Among these genes was imprinted gene, *KCNQ1,* which encodes potassium voltage-gated channel sub-family Q member 1, a key regulator of insulin secretion in β-cells. Finally, in the same cohort, maternal exposure to iAs was shown to alter diabetes-associated microRNAs in cord blood of newborns (Rager et al. 2014).

When modeling iAs-associated type 2 diabetes in laboratory settings, most studies have focused on iAs exposure in adult laboratory animals, mainly mice. Very few studies have assessed effects of prenatal exposures. In general,

Table 6 The pathways that were significantly enriched for genes ($n=95$) altered by preconception exposure to iAs in both the parental sperm and the liver of male offspring

Category	Pathway	Fold enrichment	p value	Benjamini–Hochberg adjusted p value
Gene Ontology	Extracellular matrix	16.16	1.47E−19	2.26E−17
Gene ontology	Proteinaceous extracellular matrix	15.04	6.50E−19	5.00E−17
Gene ontology	Extracellular region	3.82	8.42E−11	4.32E−09
Gene ontology	Extracellular space	3.44	1.90E−07	4.87E−06
Gene ontology	Collagen trimer	20.82	1.04E−07	3.20E−06
Gene ontology	Platelet-derived growth factor binding	90.86	1.88E−07	3.77E−05
Gene ontology	Extracellular matrix structural constituent	31.91	1.10E−06	1.11E−04
KEGG	ECM-receptor interaction	16.53	2.79E−06	2.71E−04
KEGG	Protein digestion and absorption	16.53	2.79E−06	2.71E−04
KEGG	PI3K-Akt signaling pathway	6.51	3.03E−06	1.47E−04
KEGG	Focal adhesion	9.03	3.81E−06	1.23E−04
Gene ontology	Collagen fibril organization	27.27	3.15E−05	0.010914
Gene ontology	Cellular response to amino acid stimulus	10.86	4.24E−05	0.00981
Gene ontology	Protein heterotrimerization	44.78	8.88E−05	0.012305
Gene ontology	Wound healing	15.84	4.93E−06	0.003428
Gene ontology	Cellular response to amino acid stimulus	10.86	4.24E−05	0.00981

Genes ($p<0.05$) were analyzed for pathways enrichment; the significantly enriched pathways were identified using a Benjamini–Hochberg adjusted p value <0.1

results of these studies suggest that in utero exposures alone or combined with early life exposure to low (ppb) levels of iAs in drinking water result in an increased body weight and percent fat, and produce adverse metabolic phenotypes characterized by impaired glucose and lipid metabolism in offspring, and that these effects are sex dependent (Ditzel et al. 2016; Rodriguez et al. 2016). Similarly, we have recently shown that combined preconception and in utero exposures to 100 ppb iAs lead to impaired FBG in adult male, but not female C57BL/6 offspring (Huang et al. 2018). In a recent study, Fry and associates found that the combined preconception and in utero exposures produced insulin resistance in adult male CC004 mice from the Collaborative Cross (Fry et al. 2019). In contrast, combined in utero and postnatal exposures had no effects on insulin sensitive/resistance in this mouse strain. These results suggest that the preconception exposure alone may result in a diabetic phenotype in offspring. The goal of the present study was to test this hypothesis and to explore a possibility that the effects of the preconception exposure may be associated with iAs-induced alterations in transcriptomes of the parental germ cell.

We exposed the parent mice to the environmental relevant 200 ppb iAs in drinking water. For comparison, chronic exposure to 100 ppb did not produce diabetic phenotype in adult C57BL/6 mice in our published studies (Douillet et al. 2013). We found no significant differences in diabetes indicators between the control and iAs-treated mice in the parental group. In clinical studies, diabetes during pregnancy, namely gestational diabetes, has been a risk factor for development of diabetes in offspring later in life (Damm 2009; Damm et al. 2016; Metzger 2007). A hyper-insulinogenic and hyper-glycemic fetal environment in pregnant women with diabetes, which results in fetal epigenetic re-programming of genes involved in energy metabolism is thought to drive the diabetic phenotype in the offspring (Dabelea 2007; Damm et al. 2016; Metzger 2007; Nicholas et al. 2016). The fact that in this study, dams exposed to iAs did not develop diabetes suggests that the altered phenotypes of the offspring from these dams are caused by other mechanisms.

We found that the preconception exposure to 200 ppb iAs had significant effects on diabetic indicators in C57BL/6 offspring, but these effects were strictly sex dependent. Interestingly, the 23-week-old female offspring from parents exposed to iAs prior to mating had higher % fat but lower FBG and 15-min blood glucose levels than the female offspring from the control parents. This finding seems to contradict a well-established observation that adiposity is a risk factor for diabetes in both humans and mice (Farkhondeh et al. 2019; Jeon et al. 2015; Navas-Acien et al. 2006). Notably, the preconception exposure had no significant effects on % fat, FBG or 15-min glucose levels in the male offspring. However, the higher Δ glucose$_{(15–0\text{min})}$ and Δ insulin$_{(15–0\text{min})}$ values in the male offspring from iAs-exposed parents are suggestive of an impaired glucose tolerance and insulin resistance.

To differentiate between the diabetogenic effects of fat and those of the preconception iAs exposure, we normalized the blood glucose and insulin indicators in the 23-week-old offspring and the functional indices derived from these indicators for % fat. As expected, the normalization did not eliminate the treatment-related differences in FBG and 15-min blood glucose levels of the female offspring. In fact, these differences became even more statistically significant. In addition, the difference in Δ glucose$_{(15-0\text{min})}$ also became statistically significant. Interestingly, the normalization revealed significant differences in FPI and 15-min plasma insulin levels of the female offspring; both values were lower in females from parents exposed to iAs than in those from control parents. Taken together, these results suggest that the female offspring from iAs-exposed parents, while having higher % fat, were able to manage the blood glucose levels during fasting and after glucose challenge more effectively than the female offspring from control parents, perhaps due to greater insulin sensitivity. This conclusion is further supported by our finding that the % fat-normalized HOMA-IR, the indicator of insulin resistance, was lower in females from iAs-exposed parents than in those from control parents. In comparison, in our previous study, a combined preconception and in utero exposure to 100 ppb iAs had only a marginal effect on body composition of male or female offspring and normalization for % fat eliminated significant differences in FPI and HOMA-IR between iAs-exposed and control male offspring (Huang et al. 2018). In that study, no effects of the combined exposure on diabetes indicators in female offspring were found.

Since body composition of the male offspring was not significantly affected by preconception exposure, normalizing the diabetes indicators for % fat did not change the key observations. The 15-min insulin level remained significantly higher in males from iAs-exposed parents ($p = 0.003$). The Δ insulin$_{(15-0\text{min})}$ value was also higher, but this difference did not reach statistical significance ($p = 0.07$). No difference was found in the normalized HOMA-IR. The difference in insulinogenic index, a marker of insulin secretion by β-cells in response to glucose challenge (Tura et al. 2006), which was not significant became statistically significant after normalization for % fat. The normalized insulinogenic index was significantly higher in the male offspring from iAs-exposed parents. These results indicate that the male offspring from parents exposed to iAs were able to maintain glucose homeostasis during fasting but required greater amounts of insulin to support glucose utilization after glucose challenge.

Notably, no significant effects of the preconception exposure were observed in relation to HOMA-B in male and female offspring either before or after normalizing for % fat. HOMA-B is a marker of β-cell function but is based on FBG and FPI values. Thus, it does not reflect mechanisms that are activated during glucose challenge.

Exposures to environmental contaminants have been shown to alter gene expression profiles in germ cells leading to altered phenotypes in offspring (Allegrucci et al. 2005; Bollati and Baccarelli 2010; Nilsson et al. 2018). In laboratory studies, a daily i.p. injection of iAs (6 mg/kg b.w.) for 26 days decreased testicular mass and impaired spermatogenesis in Wistar rats by increasing sperm DNA damage and decreasing testicular testosterone, epididymal sperm count, and number of germ cells at stage VII (Choudhury et al. 2011; Sarkar et al. 2003). In mice, a daily oral dose of iAs (7.5 mg/kg b.w.) for 35 days has been shown to decrease sperm motility, increased sperm morphological abnormality, and decreased sperm viability (Ferreira et al. 2012). Adverse effects of iAs have also been reported in female germ cells. For example, i.p. injection of iAs (16 mg/kg b.w.) for 14 days resulted in an increased abnormal spindle and chromosomal fragmentation in mature CD-1 oocytes at metaphase II, leading to meiotic disruption (Navarro et al. 2004). These data suggest that iAs exposure impairs structure and function of germ cells. However, associations between the iAs-induced damage to germ cells and the phenotypic outcomes in offspring remain unclear.

The present study is the first to provide evidence of a link between iAs-induced differential gene expression in germ cells and altered gene transcription profiles in tissues, particularly liver, of the offspring. Specifically, we found that many of the genes and pathways that were altered by iAs exposure in paternal sperm and maternal oocytes were also altered in the livers of male and female offspring born to the iAs-exposed parents. Notably, among these genes and pathways were those that are known to be associated with regulation of glucose homeostasis and diabetes. For example, PI3K/Akt signaling pathway and pathways are involved in maintenance and remodeling of the extracellular matrix. The PI3K/Akt signaling is activated by insulin during the postprandial stage (White and Kahn 1994). The insulin-dependent activation (phosphorylation) of Akt leads to the translocation of glucose transporter type 4 receptor (GLUT4) from the perinuclear compartment to the plasma membrane and to stimulation of glucose uptake and utilization (White and Kahn 1994). Inhibition of Akt phosphorylation or suppression of Akt expression is associated with impaired insulin signaling and insulin resistance (White and Kahn 1994). The extracellular matrix (ECM), which is composed by diverse networks of protein and proteoglycans, is involved in numerous cellular processes, including signal transduction and activation of intracellular signaling (e.g., PI3K/Akt signaling) (Williams et al. 2015). The pathways involved in maintenance and remodeling of the extracellular matrix are known to be impaired by diabetes (Law et al. 2012) and this impairment is thought to contribute to insulin resistance

(Williams et al. 2015). Notably, the diabetes-associated pathways were dysregulated in the paternal sperm as well as in the liver of male offspring, which developed the diabetic phenotype. Thus, the iAs-induced differential expression of genes in germ cells may be directly responsible for diabetic phenotype in male offspring from the iAs-exposed sires.

In summary, our results show that the preconception exposure to 200 ppb iAs in drinking water altered diabetes indicators in both male and female offspring that were not directly exposed to iAs. Notably, the effects of preconception exposure in the offspring were strictly sex specific. While the findings in the male offspring suggest an increase requirement for insulin in response to glucose challenge, the glucose and insulin indicators in the female offspring are consistent with a protective phenotype, despite increased adiposity. In addition, this study is the first to link the diabetic phenotype of the male offspring to altered gene expression in the parental germ cells. Molecular mechanisms that underlie this link will be investigated in future studies.

Acknowledgements This work was funded by the National Institutes of Health (NIH) grant R01ES028721 to M.S. and R.C.F. and the UNC Superfund Research Program Grant P42ES031007. The CGIBD is funded by the NIH Grant P30 DK034987. Additional support was provided by the UNC Institute for Environmental Health Solutions. The authors would like to thank Lauren Alexandra Eaves and Rowan Far Beck for sharing DESeq scripts, and to Madison Miller and Bingzhen Shang for their help with maintenance of the mice during the study.

Compliance with ethical standards

Conflict of interest The authors declare they have no actual or potential competing financial interests.

References

Abdul KS, Jayasinghe SS, Chandana EP, Jayasumana C, De Silva PM (2015) Arsenic and human health effects: a review. Environ Toxicol Pharmacol 40:828–846

Allegrucci C, Thurston A, Lucas E, Young L (2005) Epigenetics and the germline. Reproduction 129:137–149

Ardisson Korat AV, Willett WC, Hu FB (2014) Diet, lifestyle, and genetic risk factors for type 2 diabetes: a review from the nurses' health study, nurses' health study 2, and health professionals' follow-up study. Curr Nutr Rep 3:345–354

Beck R, Styblo M, Sethupathy P (2017) Arsenic exposure and type 2 diabetes: micrornas as mechanistic links? Curr Diab Rep 17:18

Bollati V, Baccarelli A (2010) Environmental epigenetics. Heredity (Edinburgh) 105:105–112

Carmean CM, Seino S (2019) Braving the element: pancreatic beta-cell dysfunction and adaptation in response to arsenic exposure. Front Endocrinol (Lausanne) 10:344

Castriota F, Rieswijk L, Dahlberg S, La Merrill MA, Steinmaus C, Smith MT et al (2020) A state-of-the-science review of arsenic's effects on glucose homeostasis in experimental models. Environ Health Perspect 128:16001

CDC (2020) Centers for disease control and prevention. National Diabetes Statistics Report

Choudhury SM, Gupta M, Majumder UK (2011) Toxicological potential of mycotoxin mt81 and its benzoylated derivative on testicular spermatogenesis and steroidogenesis in mature male wistar albino rats. Toxicol Mech Method 21:426–433

Chung JY, Yu SD, Hong YS (2014) Environmental source of arsenic exposure. J Prev Med Public Health 47:253–257

Dabelea D (2007) The predisposition to obesity and diabetes in offspring of diabetic mothers. Diabetes Care 30(Suppl 2):S169-174

Damm P (2009) Future risk of diabetes in mother and child after gestational diabetes mellitus. Int J Gynaecol Obstet 104(Suppl 1):S25-26

Damm P, Houshmand-Oeregaard A, Kelstrup L, Lauenborg J, Mathiesen ER, Clausen TD (2016) Gestational diabetes mellitus and long-term consequences for mother and offspring: a view from denmark. Diabetologia 59:1396–1399

Dennis G Jr, Sherman BT, Hosack DA, Yang J, Gao W, Lane HC et al (2003) David: database for annotation, visualization, and integrated discovery. Genome Biol 4:P3

Ditzel EJ, Nguyen T, Parker P, Camenisch TD (2016) Effects of arsenite exposure during fetal development on energy metabolism and susceptibility to diet-induced fatty liver disease in male mice. Environ Health Perspect 124:201–209

Dobin A, Davis CA, Schlesinger F, Drenkow J, Zaleski C, Jha S et al (2013) Star: ultrafast universal rna-seq aligner. Bioinformatics 29:15–21

Douillet C, Currier J, Saunders J, Bodnar WM, Matousek T, Styblo M (2013) Methylated trivalent arsenicals are potent inhibitors of glucose stimulated insulin secretion by murine pancreatic islets. Toxicol Appl Pharm 267:11–15

Dover EN, Beck R, Huang MC, Douillet C, Wang Z, Klett EL et al (2018a) Arsenite and methylarsonite inhibit mitochondrial metabolism and glucose-stimulated insulin secretion in ins-1 832/13 beta cells. Arch Toxicol 92:693–704

Dover EN, Patel NY, Styblo M (2018b) Impact of in vitro heavy metal exposure on pancreatic beta-cell function. Toxicol Lett 299:137–144

Farkhondeh T, Samarghandian S, Azimi-Nezhad M (2019) The role of arsenic in obesity and diabetes. J Cell Physiol 234:12516–12529

Ferreira M, Matos RC, Oliveira H, Nunes B, Pereira MD (2012) Impairment of mice spermatogenesis by sodium arsenite. Hum Exp Toxicol 31:290–302

Fry RC, Addo KA, Bell TA, Douillet C, Martin E, Styblo M et al (2019) Effects of preconception and in utero inorganic arsenic exposure on the metabolic phenotype of genetically diverse collaborative cross mice. Chem Res Toxicol 32:1487–1490

Grau-Perez M, Kuo CC, Gribble MO, Balakrishnan P, Jones Spratlen M, Vaidya D et al (2017) Association of low-moderate arsenic exposure and arsenic metabolism with incident diabetes and insulin resistance in the strong heart family study. Environ Health Perspect 125:127004

Huang DW, Sherman BT, Lempicki RA (2009) Systematic and integrative analysis of large gene lists using david bioinformatics resources. Nat Protoc 4:44–57

Huang MC, Douillet C, Dover EN, Styblo M (2018) Prenatal arsenic exposure and dietary folate and methylcobalamin supplementation alter the metabolic phenotype of c57bl/6j mice in a sex-specific manner. Arch Toxicol 92:1925–1937

Huang M, Douillet C, Styblo M (2019) Arsenite and its trivalent methylated metabolites inhibit glucose-stimulated calcium influx and insulin secretion in murine pancreatic islets. Arch Toxicol 93:2525–2533

Jeon JY, Ha KH, Kim DJ (2015) New risk factors for obesity and diabetes: Environmental chemicals. J Diabetes Investig 6:109–111

Kapaj S, Peterson H, Liber K, Bhattacharya P (2006) Human health effects from chronic arsenic poisoning—a review. J Environ Sci Health A Toxic Hazard Subst Environ Eng 41:2399–2428

Kile ML, Houseman EA, Baccarelli AA, Quamruzzaman Q, Rahman M, Mostofa G et al (2014) Effect of prenatal arsenic exposure on DNA methylation and leukocyte subpopulations in cord blood. Epigenetics 9:774–782

Lai MS, Hsueh YM, Chen CJ, Shyu MP, Chen SY, Kuo TL et al (1994) Ingested inorganic arsenic and prevalence of diabetes mellitus. Am J Epidemiol 139:484–492

Law FV, Goldsmith JG, Carver W, Goldsmith EC (2012) Diabetes-induced alterations in the extracellular matrix and their impact on myocardial function. Microsc Microanal 18:22–34

Liu S, Guo X, Wu B, Yu H, Zhang X, Li M (2014) Arsenic induces diabetic effects through beta-cell dysfunction and increased gluconeogenesis in mice. Sci Rep 4:6894

Love MI, Huber W, Anders S (2014) Moderated estimation of fold change and dispersion for RNA-seq data with deseq2. Genome Biol 15:550

Martin EM, Styblo M, Fry RC (2017) Genetic and epigenetic mechanisms underlying arsenic-associated diabetes mellitus: a perspective of the current evidence. Epigenomics 9:701–710

Maull EA, Ahsan H, Edwards J, Longnecker MP, Navas-Acien A, Pi J et al (2012) Evaluation of the association between arsenic and diabetes: a national toxicology program workshop review. Environ Health Perspect 120:1658–1670

Metzger BE (2007) Long-term outcomes in mothers diagnosed with gestational diabetes mellitus and their offspring. Clin Obstet Gynecol 50:972–979

Naujokas MF, Anderson B, Ahsan H, Aposhian HV, Graziano JH, Thompson C et al (2013) The broad scope of health effects from chronic arsenic exposure: update on a worldwide public health problem. Environ Health Perspect 121:295–302

Navarro PA, Liu L, Keefe DL (2004) In vivo effects of arsenite on meiosis, preimplantation development, and apoptosis in the mouse. Biol Reprod 70:980–985

Navas-Acien A, Silbergeld EK, Streeter RA, Clark JM, Burke TA, Guallar E (2006) Arsenic exposure and type 2 diabetes: a systematic review of the experimental and epidemiologic evidence. Environ Health Persp 114:641–648

Navas-Acien A, Silbergeld EK, Pastor-Barriuso R, Guallar E (2008) Arsenic exposure and prevalence of type 2 diabetes in us adults. JAMA 300:814–822

Nicholas LM, Morrison JL, Rattanatray L, Zhang S, Ozanne SE, McMillen IC (2016) The early origins of obesity and insulin resistance: timing, programming and mechanisms. Int J Obes 40:229–238

Nilsson EE, Sadler-Riggleman I, Skinner MK (2018) Environmentally induced epigenetic transgenerational inheritance of disease. Environ Epigenet 4:dvy016

Padmaja Divya S, Pratheeshkumar P, Son YO, Vinod Roy R, Andrew Hitron J, Kim D et al (2015) Arsenic induces insulin resistance in mouse adipocytes and myotubes via oxidative stress-regulated mitochondrial sirt3-foxo3a signaling pathway. Toxicol Sci 146:290–300

Paul DS, Hernandez-Zavala A, Walton FS, Adair BM, Dedina J, Matousek T et al (2007) Examination of the effects of arsenic on glucose homeostasis in cell culture and animal studies: Development of a mouse model for arsenic-induced diabetes. Toxicol Appl Pharmacol 222:305–314

Paul DS, Walton FS, Saunders RJ, Styblo M (2011) Characterization of the impaired glucose homeostasis produced in c57bl/6 mice by chronic exposure to arsenic and high-fat diet. Environ Health Perspect 119:1104–1109

Rager JE, Bailey KA, Smeester L, Miller SK, Parker JS, Laine JE et al (2014) Prenatal arsenic exposure and the epigenome: altered micrornas associated with innate and adaptive immune signaling in newborn cord blood. Environ Mol Mutagen 55:196–208

Rahman M, Tondel M, Ahmad SA, Axelson O (1998) Diabetes mellitus associated with arsenic exposure in bangladesh. Am J Epidemiol 148:198–203

Rodriguez KF, Ungewitter EK, Crespo-Mejias Y, Liu C, Nicol B, Kissling GE et al (2016) Effects of in utero exposure to arsenic during the second half of gestation on reproductive end points and metabolic parameters in female cd-1 mice. Environ Health Perspect 124:336–343

Rojas D, Rager JE, Smeester L, Bailey KA, Drobna Z, Rubio-Andrade M et al (2015) Prenatal arsenic exposure and the epigenome: Identifying sites of 5-methylcytosine alterations that predict functional changes in gene expression in newborn cord blood and subsequent birth outcomes. Toxicol Sci 143:97–106

Romao I, Roth J (2008) Genetic and environmental interactions in obesity and type 2 diabetes. J Am Diet Assoc 108:S24-28

Sarkar M, Chaudhuri GR, Chattopadhyay A, Biswas NM (2003) Effect of sodium arsenite on spermatogenesis, plasma gonadotrophins and testosterone in rats. Asian J Androl 5:27–31

Thayer KA, Heindel JJ, Bucher JR, Gallo MA (2012) Role of environmental chemicals in diabetes and obesity: a national toxicology program workshop review. Environ Health Perspect 120:779–789

Tseng CH (2004) The potential biological mechanisms of arsenic-induced diabetes mellitus. Toxicol Appl Pharmacol 197:67–83

Tseng CH, Tai TY, Chong CK, Tseng CP, Lai MS, Lin BJ et al (2000) Long-term arsenic exposure and incidence of non-insulin-dependent diabetes mellitus: a cohort study in arseniasis-hyperendemic villages in taiwan. Environ Health Perspect 108:847–851

Tura A, Kautzky-Willer A, Pacini G (2006) Insulinogenic indices from insulin and C-peptide: comparison of beta-cell function from OGTT and IVGTT. Diabetes Res Clin Pract. 72:298–301

Venkatratnam A, House JS, Konganti K, McKenney C, Threadgill DW, Chiu WA et al (2018) Population-based dose-response analysis of liver transcriptional response to trichloroethylene in mouse. Mamm Genome 29:168–181

Walton FS, Harmon AW, Paul DS, Drobna Z, Patel YM, Styblo M (2004) Inhibition of insulin-dependent glucose uptake by trivalent arsenicals: Possible mechanism of arsenic-induced diabetes. Toxicol Appl Pharmacol 198:424–433

White MF, Kahn CR (1994) The insulin signaling system. J Biol Chem 269:1–4

WHO (2017) Guidelines for drinking-water quality. World Health Organization

Williams AS, Kang L, Wasserman DH (2015) The extracellular matrix and insulin resistance. Trends Endocrinol Metab 26:357–366

Zhang C, Fennel EMJ, Douillet C, Styblo M (2017) Exposures to arsenite and methylarsonite produce insulin resistance and impair insulin-dependent glycogen metabolism in hepatocytes. Arch Toxicol 91:3811–3821